Energy levels of ^{249}Cm from measurements of thermal neutron capture gamma rays

R. W. Hoff
University of California, Lawrence Livermore Laboratory, Livermore, California 94550

W. F. Davidson,* D. D. Warner,† H. G. Börner, and T. von Egidy‡
Institut Laue-Langevin, 38042 Grenoble, France
(Received 20 July 1981)

The excited levels of ^{249}Cm have been determined by use of neutron-capture gamma-ray spectroscopy. Gamma-ray measurements were made with curved-crystal spectrometers of focal lengths 5.8 and 24 m and a pair spectrometer. These experimental data represent the first measurement of gamma transitions depopulating the levels of ^{249}Cm. We present evidence for the population of 23 levels in ^{249}Cm up to 1300-keV excitation. The following new configuration assignments were made (listed with the corresponding bandhead energies): $\frac{5}{2}^{+}$[622], 529.58 keV; $\frac{3}{2}^{-}$[752], 772.74 keV; $\frac{1}{2}^{-}$[501], 917.49 keV. Comparison of the experimentally determined level structure with theoretical calculations shows best agreement with calculations by Soloviev's group where a Woods-Saxon potential form was used and quasiparticle-phonon coupling was included. The neutron binding energy was determined to be 4713.7 ± 0.3 keV.

[NUCLEAR REACTIONS ^{248}Cm(n,γ), E = thermal; measured E_γ, I_γ, ^{249}Cm deduced levels, J, π, Nilsson assignments.]

I. INTRODUCTION

An extensive body of experimental nuclear structure data has been collected that demonstrates that the mass region $255 > A > 225$ is comprised of nuclei with stable quadrupole deformation. Various techniques of experimental nuclear spectroscopy have been employed to map the excited levels of these nuclei. These data are interpreted in terms of single-particle excitations, collective motion such as rotation and vibration, and interactions between these two distinct modes of nuclear excitation.[1,2] The nucleus ^{249}Cm is close to the upper edge of a region of nuclei where precise nuclear spectroscopic techniques can be applied. With increasing mass number, the nuclides in this region become more unstable, especially toward spontaneous fission, and half-lives become extremely short. Level structure has not been investigated in very much detail beyond about $A = 251$. Either there is insufficient target material available to produce heavier nuclides or the intense radioactivity of heavy targets makes the experiments impractical.

The ^{248}Cm target material used in our measurements is the product of alpha decay of hundreds of milligrams of ^{252}Cf. This californium was produced in relatively large quantities through long-term neutron irradiations of plutonium at high flux levels. As a part of the U.S. national effort to produce transplutonic elements for research purposes, available stocks of ^{252}Cf at Oak Ridge National Laboratory have been purified and stored to allow for alpha decay to ^{248}Cm. The daughter curium is periodically separated from the parent ^{252}Cf. Since the alpha decay rate of ^{252}Cf greatly exceeds that of other Cf isotopes present, the daughter curium is largely ^{248}Cm.

The neutron capture gamma ray spectroscopy facility at Institut Laue-Langevin is ideally suited for the study of targets made of rare materials and with low capture cross sections. The intense thermal neutron flux at the target position, 5.5×10^{14} neutrons/cm^2 sec, and the high resolution of the curved-crystal gamma ray spectrometers and the beta-ray spectrometer are the principal features of this facility. Even at this neutron flux level, we still encountered some experimental limitations owing to the low capture cross section of ^{248}Cm, the fissionability of the capture products, and consequent problems with both heat dissipation in the target and interference in the gamma-ray spectrum from fission product lines. Nevertheless, we were able to apply the inherently excellent resolution of the curved-crystal spectrometers to an investigation of the level structure of ^{249}Cm.

Prior to our measurements, the level structure of ^{249}Cm had been the subject of two experimental investigations. Most of the information already known comes from a charged particle reaction spectroscopy experiment that involved the ^{248}Cm$(d,p)^{249}$Cm reaction.[3] In the alpha decay of ^{253}Cf, only two alpha groups populating levels of ^{249}Cm have been observed.[4] Our measurements of the gamma ray transitions accompanying neutron capture provide significant new knowledge of the ^{249}Cm level structure,[5] especially because transitions between levels were not measured in either of the previous studies.

II. EXPERIMENTAL

The experiments were performed with the GAMS 1, GAMS 2/3, and pair spectrometers at the high flux reactor of the Institut Laue-Langevin at Grenoble. All three gamma-ray spectrometers are installed at the same through tube and are viewing the same target.

A. Crystal spectrometers

1. Target

The target material used was ^{248}Cm of high isotopic purity; results of an isotopic analysis are shown in Table I. Chemically, it was relatively pure CmO_2, although we observed some capture gamma lines indicating that Sm and Nd isotopes were present as minor impurities (at a concentration of a few tens of ppm). The target contained 54 mg of ^{248}Cm and was fabricated in the form of a rectangular wafer, $29\times5\times0.20$ mm, surrounded by aluminum as containment material. The overall dimensions of the oxide-aluminum wafer were $40\times6\times0.36$ mm. This wafer was mounted in a graphite holder and was suspended in the center of the through tube in the reactor where the thermal flux level was 5.5×10^{14} neutrons/cm^2 sec. This GAMS target configuration is described in greater detail in Ref. 6.

2. Spectrometers

Secondary gamma rays emitted from this target were measured by use of two curved-crystal spectrometers,[6] GAMS 1 and GAMS 2/3. The target is viewed end on by the two spectrometers, from opposite ends of the through tube.

GAMS 1 is a 5.8 m, curved-crystal spectrometer arranged in Dumond geometry. Gamma rays are diffracted by the 110 planes of a 4 mm thick quartz crystal. The diffraction angle is measured by means of laser-based Michelson angle interferometry. The Bragg-reflected gamma rays are detected by a 5×5 cm NaI(Tl) detector. The first five orders of reflection are recorded simultaneously. With the ^{248}Cm target, a resolution described by the equation E (keV)$=2.2\times10^{-5}E^2$ (keV)$/n$ was obtained, where n is the reflection order; this corresponds to 100 eV FWHM at 100 keV when observed in second order. This resolution was entirely determined by the target thickness and was about ten times the best obtainable value. This was due partly to the thickness of the target (0.2 mm) and partly to the nonplanar character of the wafer.

The curved-crystal spectrometer GAMS 2/3 has a focal length of 24 m, and features two quartz crystals which have a common axis of rotation and

TABLE I. Isotopic composition and capture rates for the ^{248}Cm target.

Mass number	Abundance (at. %)	Thermal neutron capture cross section (b)	Fraction of total neutron capture rat (%)
243	<0.0003	225.0	<0.018
244	0.002	10.0	0.005
245	0.058	343.0	5.39
246	3.32	1.3	1.12
247	0.0017	60.0	0.28
248	96.60	3.6	93.18

which diffract to either side of the incident gamma-ray beam. The spectrometer is operated so that each gamma line is scanned simultaneously on both sides of the instrument; thus, one can obtain an angle of diffraction, $\theta=(\theta_1+\theta_2)/2$, that is independent of the source position. In this spectrometer we obtained a resolution described by the equation E (keV)$=5.6\times10^{-6}E^2$ (keV)$/n$; this corresponds to 170 eV FWHM at 300 keV when observed in third order. This spectrometer was used to scan the spectrum in the energy range 100−1500 keV.

Measurements were taken over a 22-d period, during which three successive scans of the energy ranges of the spectrometers were made.

Since the reflection coefficient for a quartz crystal decreases for higher orders of reflectivity, only the more intense lines are observed in the higher-order spectra. Nevertheless, the reported transitions were observed in several spectra representing various orders of reflectivity in separate spectrometers. This redundancy provides for good reliability and accuracy in the measured energies and intensities for each transition.

B. Pair spectrometer

Primary gamma rays in the energy range 2−6 MeV were measured by use of a Ge(Li) pair spectrometer which views the target at distance of 17 m. This spectrometer consists of a 7 cm^3 planar Ge(Li) detector (FWHM $=4.3$ keV at $E_\gamma=6.6$ MeV) that is surrounded by two 15.2×10.2 cm NaI(Tl) detectors for detection of the 511 keV annihilation quanta. Several spectra were collected at intervals during the 22-d irradiation. Thus, the intensities of gamma rays observed with this spectrometer could be checked for time dependence over the measurement period.

III. RESULTS

The absolute energies of the ^{249}Cm secondary gamma lines were calibrated with a selected set of 44 fission-product gamma-ray energies[7] (70−900 keV) which, in turn, were linked to a value of 411.8042 keV for the ^{198}Au decay line.[8] Precise energies and intensities for Cm and Bk K x rays have been derived and will be published elsewhere.[9]

Gamma ray intensities of the ^{249}Cm lines were derived from the observed peak areas by correcting for self-absorption in the target, for absorption in the through tube and windows, for reflectivity in the quartz crystal, and for detection efficiency in the NaI detectors (see also Ref. 6).

The gamma lines measured by use of the curved-crystal spectrometers and assigned to ^{248}Cm$(n,\gamma)^{249}$Cm are listed in Table II.

Since ^{248}Cm has a relatively low neutron capture section, the ^{248}Cm capture rate was essentially constant during the irradiation. The gamma rays observed in our experiment can arise from a number of sources other than neutron capture in ^{248}Cm. The most important source of extraneous gamma rays in the energy range below 1500 keV is neutron-induced fission. This rate of fission did not change appreciably with time. At the beginning of the irradiation, ^{245}Cm was an important source of fission (see Table I). As the initial amount of ^{245}Cm decreased (it is destroyed with an effective half-life of seven days by virtue of its 2070 b cross section), other nuclides, e.g., ^{249}Cf and ^{250}Bk, which are products of successive neutron capture reactions and beta decay, contributed appreciably to the fission rate. In our experiments we observe about 100 lines whose energies match with precisely-measured fission product energies reported previously[7] and which have been eliminated from the ^{248}Cm$(n,\gamma)^{249}$Cm list.

We have identified the most intense gamma transitions from the beta decay of two capture products, 65-min ^{249}Cm and 3.2-h ^{250}Bk; these transitions are listed in Table III. Since absolute intensities for the two gamma transitions in ^{249}Cm beta decay are known,[10] our intensities are linked to these transitions in order to get γ intensity per neutron capture. Other curium isotopes in the target did not produce significant capture reactions, with the possible exception of ^{245}Cm. Its capture rate was 0.06 times that of ^{248}Cm at the beginning of the irradiation. Owing to rapid destruction, the rate was down to 0.01 times that of ^{248}Cm after 16 d. Since the ^{248}Cm capture rate was essentially constant over the entire period of the irradiation, the time dependence of the gamma rays served to eliminate ^{245}Cm(n,γ) contributions. The list of secondary gamma rays was checked for interference from the ^{249}Bk$(n,\gamma)^{250}$Bk reaction by comparing with spectra obtained from a ^{249}Bk target used in a separate measurement; the ^{249}Bk in our Cm target is the product of ^{249}Cm beta decay.

A. Pair spectrometer results

A prominent feature of the spectra taken with the pair spectrometer is a large set of intense gamma

TABLE II. Gamma ray transitions from the ^{248}Cm$(n,\gamma)^{249}$Cm reaction measured by use of the GAMS 1 and GAMS 2/3 spectrometers.

E (keV)	ΔE (eV)	I_γ (phot/1000 capt)	ΔI_γ	Assignment
40.111	7	17.8	7.0	
40.146	6	20.0	7.0	
41.554	4	15.0	1.5	
57.963	6	17.4	3.3	
58.060	8	14.8	3.7	
59.282	5	43.2	6.1	
59.368	7	24.9	5.7	
65.139	8	11.3	3.2	
66.808	10	15.3	3.0	
66.901	10	10.0	2.3	
67.209	11	9.1	2.5	
68.179	14	7.8	2.8	
75.736	3	14.4	2.3	
75.865	76	8.2	2.0	
76.647	4	6.3	1.3	546.9-470.2
				1047.8-971.2
78.392	5	6.4	1.7	1153.5-971.2
83.922	7	4.1	1.2	110.2- 26.2
84.700	6	6.4	1.4	1047.8-963.0
97.799[a]	10	4.4	0.7	208.0-110.2
100.395	12	2.9	0.9	
102.664[a]	7	37.5	5.7	
102.783	8	28.7	4.0	
111.113	16	2.4	0.7	
114.859	32	7.8	1.2	
115.064	45	15.6	2.3	
115.306	50	4.5	0.8	
116.338[a]	15	2.8	1.0	
116.775	25	3.8	0.9	
117.706	7	4.8	0.8	
125.061	16	5.3	1.9	
126.897	49			
129.149[a]	20	8.3	3.3	
129.862	15	10.9	4.0	
130.260	12	15.3	4.3	1047.8-917.5
133.659	27	13.6	5.7	
137.190	43	6.3	0.8	
137.822	14	11.3	2.4	
138.360	14	8.7	1.6	
146.479	19	7.7	2.2	
147.842[a]	27	4.0	1.9	
148.155	18	5.7	1.3	
149.738	9	4.6	0.7	
150.266	16	9.9	1.8	
153.846	28	3.9	1.4	
158.544	33	9.9	1.9	
158.879[a]	17	5.3	0.5	
159.215	21	9.9	2.4	208.0- 48.7
159.765	16	9.0	1.8	208.0- 48.2
161.391	30	6.3	1.1	
162.314	14	8.0	0.9	
165.823	24	5.7	0.7	
167.650	40	4.9	0.7	
171.585	14	8.7	1.1	
181.778	11	10.3	2.2	208.0- 26.2
182.146[a]	43	3.0	0.3	1153.5-971.2
193.24[a]	59	5.5	1.3	242.0- 48.7
193.805	20	8.0	1.2	242.0- 48.2
194.334	43	2.2	0.3	
198.945[a]	56	2.2	0.3	
208.011	7	15.8	2.2	208.0- 0.0
214.977[a]	39	3.4	1.0	
216.531	51	2.7	0.9	
218.702	23	5.7	1.1	
225.942	73	4.2	1.4	772.8-546.9
227.375	34	2.4	0.6	
228.949[a]	34	3.1	0.5	1047.8-818.9
229.343	25	2.0	0.3	
230.638[a]	54	7.9	2.2	
236.780	45	4.8	1.3	
240.253	9	5.9	0.9	289.0- 48.7
240.451	10	3.0	0.6	818.9-578.4
240.618	15	11.8	2.0	529.6-289.0
240.780	20	9.3	1.7	289.0- 48.2
242.011	76	2.8	0.4	242.0- 0.0
257.742[a]	51	16.1	5.1	546.9-289.0
265.721	57	4.6	0.9	
267.163	33	13.1	3.3	
269.671	28	12.3	2.4	
269.910	30	12.2	2.1	
272.039	49	2.2	1.3	818.9-546.9
275.388	23	7.3	1.4	
278.229	69	3.2	1.0	772.8-494.5
280.769[a]	41	9.0	2.3	
302.589	65	8.5	2.8	772.8-470.2
307.39[a]	190	3.2	1.4	
312.120	16	5.3	1.3	859.0-546.9
314.161	44	6.7	1.8	
316.329	50	6.0	1.4	
321.891[a]	418	3.7	2.5	529.6-208.0
339.23	120	4.1	1.1	546.9-208.0
340.009	97	11.5	3.0	
340.369	10	10.4	1.9	
343.021	96	6.0	1.3	
343.167	70	4.8	1.6	
348.748	37	7.2	1.9	818.9-470.2
349.560	95	5.2	1.5	
349.827	14	6.6	1.4	
353.772	58	3.9	1.1	
357.68[a]	170	5.6	1.6	
366.69	110	7.2	2.9	
373.887	33	4.8	1.5	
400.203	48	11.9	1.2	

TABLE II. (*Continued.*)

E (keV)	ΔE (eV)	I_γ (phot/1000 capt)	ΔI_γ	Assignment	E (keV)	ΔE (eV)	I_γ (phot/1000 capt)	ΔI_γ	Assignment
400.398	55	14.3	2.7		830.70	60	46.3	6.3	
400.583	43	16.9	3.5		831.06	50	49.6	14.9	
400.820	35	13.0	2.5		832.70	100	24.3	4.1	859.0-26.2
401.63	160	6.7	0.6		846.23	250	59.3	12.4	
415.07	140	4.4	1.1		860.80	130	12.4	3.0	971.2-110.2
418.07	140	3.3	1.1		861.39	240	9.4	1.9	
422.015	6	35.9	6.2	470.2-48.2	891.25	210	12.7	3.9	917.5-26.2
422.94	100	7.4	1.9	917.5-494.5	899.92	90	14.1	3.0	
434.009[a]	62	5.8	0.6		914.74	110	14.3	3.3	963.2-48.2
441.55	110	2.8	0.8	971.2-529.6	941.96	100	36.4	9.4	
444.095[a]	80	2.5	0.8	470.2-26.2	957.63	210	7.7	1.9	
447.308	72	4.4	1.4	917.5-470.2	963.06	90	8.0	1.9	963.2-0.0
452.36	110	2.5	1.1		968.23	120	15.2	4.4	1175.9-208.0
468.259	8	20.8	3.5	578.4-110.2	981.68	110	80	17	
				494.5-26.2	982.13	100	93	18	
470.198	9	30.0	7.4	470.2-0.0	983.06	30	117	22	
490.56	160	3.3	1.1		983.92	80	83	14	
494.484	3	27.2	6.0	494.5-0.0	1012.19	120	52	9	
497.384	59	6.6	1.7		1013.69	50	88	16	
505.95	30	11.0	3.9		1014.87	130	50	8	
524.55	50	10.5	2.5		1073.59	190	17	3	
531.72[a]	530	10.0	1.0	772.8-242.0	1127.37	220	22	4	1153.5-26.2
535.55	50	7.7	1.1		1135.01	240	28	4	
539.36[a]	190	9.7	1.0		1175.78	260	21	4	1175.9-0.0
548.63[a]	130	5.3	1.4		1186.71	210	40	7	
550.30	20	11.9	1.7		1193.67	270	22	4	
575.58	70	3.6	0.8		1225.21	490	30	7	
588.92	30	18.6	3.6		1239.76	470	15	4	
589.84	130	9.6	1.9		1252.34	320	22	4	
602.24[a]	60	8.5	1.7		1269.50	150	38	8	1269.5-0.0
606.73	140	3.0	0.8	1153.5-546.9	1278.95	340	28	6	
621.59[a]	330	12.3	2.2		1283.46	190	92	15	
630.19	80	8.0	1.9		1284.78	340	30	6	
658.45	60	9.9	3.0		1313.51	140	32	6	
683.35	160	3.0	1.1	1153.5-470.2	1334.56	230	36	7	
705.65	50	10.2	3.3	1175.9-470.2	1342.02	170	26	5	
724.44[a]	70	22.3	6.9	772.8-48.2	1365.19	510	27	7	
743.07	50	11.0	2.2		1408.28	300	195	28	
772.80[a]	100	12.4	3.3	772.8-0.0	1435.74	490	34	9	
778.44	110	6.3	1.7		1480.06	340	12	3	
786.29	120	27.8	4.4		1525.72	300	81	14	
787.35[a]	150	6.9	2.2		1590.5	1200	57	17	
819.58	50	16.8	3.3		1622.91	130	161	29	

[a]The existence for these transitions must be considered tentative.

transitions that arise from the $^{27}Al(n,\gamma)^{28}Al$ reaction in the aluminum used to contain the CmO_2. The stronger lines in this spectrum, along with a carbon line at 4945 keV which also arises from reactions in structural material of the target assembly, were used to calibrate the spectrometer. Energies of the aluminum capture lines were taken from Ishaq *et al.*[11] A comprehensive list of aluminum lines, including the data of Ref. 11 plus those of Stelts and Chrien[12] for the less intense lines, were used to eliminate interference in the ^{248}Cm primary spectrum. The remaining gamma rays that we observed

TABLE III. Gamma ray transitions from beta decay of ^{249}Cm and ^{250}Bk measured by use of the GAMS 1 and GAMS 2/3 spectrometers.

	Neutron capture measurements				Beta decay measurements[a]				
	E (keV)	ΔE (eV)	I_γ (photons/1000 captures)	ΔI_γ	E (keV)	ΔE (eV)	I_γ (photons/1000 beta decays)	ΔI_γ	Remarks
^{249}Cm	137.190	43	6.3	0.8	136.90	60	0.39	0.03	Abundance, energy do not match
	368.571	26	7.0	0.9	368.76	60	3.5	0.2	Also fission product, ^{104}Nb
	Not detected				518.48	60	0.88	0.06	
	560.485	26	8.5	2.2	560.39	60	8.4	0.6	^{249}Cm intensity calibration line
	621.59	330	5.3	1.0	621.87	60	1.82	0.13	(n,γ) observation too intense
	634.311	19	14.8	0.7	634.31	60	15.0	1.0	^{249}Cm intensity calibration line
	Not detected				652.80	60	1.43	0.10	
						(relative intensities)			
^{250}Bk	Not detected				889.956	22	3.40	0.5	
	Not detected				929.468	22	2.74	0.4	
	989.225	17	210	40	989.125	21	100.0		
	1028.1	400	14	4	1028.654	25	10.9	0.3	
	1031.921	25	140	27	1031.852	21	79.1	1.2	

[a]Gamma rays from beta decay of ^{249}Cm and ^{250}Bk were taken from Ref. 10.

in the energy range 3400–4713 keV are listed in Table IV. This list has been checked for interferences from the ^{249}Bk$(n,\gamma)^{250}$Bk reaction. The list in Table IV was also checked for fission product gamma lines, as summarized in the lists published by Blachot *et al.*[13] Of the 17 lines listed in the table, eleven are assigned to primary transitions that populate levels whose existence in ^{249}Cm is substantiated by the observation of secondary gamma rays as well.

Assuming the 4713.4 keV transition populates the ground state and averaging over additional primary transitions placed in the level scheme (see Sec. IV), the neutron binding energy in ^{248}Cm was determined to be 4713.7 $\pm$0.4 keV. The error includes a systematic error of 0.3 keV in the aluminum capture data of Ishaq *et al.*[11] This result is in agreement with the value (4713$\pm$6 keV) of Wapstra and Bos.[14]

IV. LEVEL SCHEME

A. Model-independent scheme

Using the gamma ray data listed in Tables II and IV, we have constructed a model-independent level scheme for ^{249}Cm as shown in Fig. 1. As a basis for construction, we have taken a series of levels below 300 keV that are populated by the ^{248}Cm$(d,p)^{249}$Cm reaction and were observed experimentally by Braid *et al.*[3] The first four of these, at 0, 25$\pm$2, 48$\pm$1, and 110$\pm$1 keV, were assigned as the lowest-lying members of a $K^\pi=\frac{1}{2}^+$ band. Three other levels, at 208$\pm$1, 242$\pm$1, and 288$\pm$5 keV, were assigned as the lowest-lying members of a $K^\pi=\frac{3}{2}^+$ rotational band. The existence of all these levels is corroborated by our observations and we have obtained a more precise energy for each. We have assumed the spin and parity assignments for these levels as proposed by Braid *et al.*[3] In the following, Ref. 3 will be abbreviated as BCEF.

Primary transitions, those which originate from the decay of the initial capture state, provide important evidence for the existence of excited levels. Having measured the neutron binding energy in ^{249}Cm, we obtain excited level energies directly from the high-energy gamma spectrum. We consider as strong evidence for the existence of a level the observation of a primary transition plus multiple secondary gamma rays that feed into the lower-lying level structure which has already been determined experimentally. Experience has shown that

TABLE IV. High-energy gamma rays in ^{249}Cm pair spectrometer measurement.[a]

Gamma ray energy[a] (keV)	Relative intensity	Implied level energy in ^{249}Cm (keV)[b]	Remarks
4713.4(4)	8.6(7)	0	
4505.0(3)	12.4(8)	208.4(5)	
4406.5(4)	7.5(7)	[306.8(6)]	
4243.5(3)	35.2(16)	469.9(5)	
4219.0(3)	57.1(24)	494.4(5)	
4022.9(4)	12.9(12)	[690.5(6)]	Complex
3854.5(8)	5.5(21)	858.8(9)	Doubtful
3796.1(3)	21.2(12)	917.3(5)	
3750.7(3)	61.7(27)	962.7(5)	
3702.1(4)	9.2(8)	[1011.3(6)]	
3663.5(3)	29.5(18)	1049.9(5)	
3560.6(10)	36.3(45)	1152.8(11)	Interference from ^{27}Al(n,γ)
3538.3(3)	100.0(4)	1175.0(5)	
3509.7(3)	37.9(19)	[1203.6(5)]	
3450.1(5)	6.7(13)	[1263.3(6)]	Doubtful
3444.9(3)	72.9(33)	1268.5(5)	
3399.0(4)	10.5(11)	[1314.4(6)]	

[a]The data listed in this column are transition energies that have been corrected for nuclear recoil energy.
[b]Level energies are listed only for those gamma rays that can be assigned to ^{249}Cm decay, i.e., for those transitions where there is no question of fission product interference or assignment to ^{249}Bk$(n,\gamma)^{250}$Bk. The level energies listed in brackets are not substantiated by observation of secondary gamma rays feeding or depopulating the level.

the most intense primary gammas are often $E1$ transitions. Thus, spin assignments of $I^{\pi}=\frac{1}{2}^-, \frac{3}{2}^-$ are favored for levels populated by intense primary gamma rays. In addition, we assume that the secondary transitions we observe are of either $E1$, $M1$, or $E2$ multipolarity. Since energies of many of the secondary gamma transitions have been measured precisely, we make use of the Ritz combination principle to define some levels. The level energies in Fig. 1 were calculated by making a least-squares fit to the transition energies.

The following is a discussion of certain details that comprise the evidence for the level scheme of Fig. 1. A list of transitions depopulating each level is given in Table VII.

Levels at 0, 26.24, and 48.20 keV. These levels were assigned previously[3] to have even parity with a spin sequence of $\frac{1}{2}$, $\frac{3}{2}$, and $\frac{5}{2}$. Our results agree with that assignment. We observe a weak primary transition (4713.4±0.4 keV) to the ground state of ^{249}Cm. A possible primary transition to the $I=\frac{3}{2}$ level at 26.24 keV cannot be determined because of the presence of an intense aluminum capture line at 4690.9 keV.

Level at 48.74 keV. The evidence for this level consists of three gamma transitions from levels at 208.00, 242.00, and 288.97 keV. Based upon these populating transitions from a band of levels whose spins and parities are known, possible spin and parity assignments for this 48.74 keV level are $\frac{3}{2}^+$, $\frac{5}{2}$, and $\frac{7}{2}^+$.

Level at 110.17 keV. The (d,p) measurements of BCEF have provided good evidence for a level(s) at 110 keV. The $I=\frac{7}{2}$ member of the ground state band is calculated to appear at 109.42 keV, based upon rotational constants derived from the lower spin levels. The best candidate for a possible $M1$ or $E2$ transition deexciting this $I=\frac{7}{2}$ level is an 83.922±0.007 keV gamma ray which is assigned to the $E2$ transition leading to the 26.24 keV $I=\frac{3}{2}$ level. Based upon this placement, we define a level at 110.17 keV which will subsequently be shown to be populated by three transitions from higher-lying levels. The (d,p) experiments have been interpreted to indicate an $I=\frac{9}{2}$ level at 110 keV, also. It is unlikely that we would see any transitions to or from this level in our experiment.

Levels at 208.00, 242.00, and 288.97 keV. The 208.00 keV level is populated by a primary transition. All three levels are well established on the basis of several transitions that populate and depopulate the levels. These levels are assumed to have even parity with a spin sequence of $\frac{3}{2}$, $\frac{5}{2}$, $\frac{7}{2}$ based on the previous assignment by BCEF.

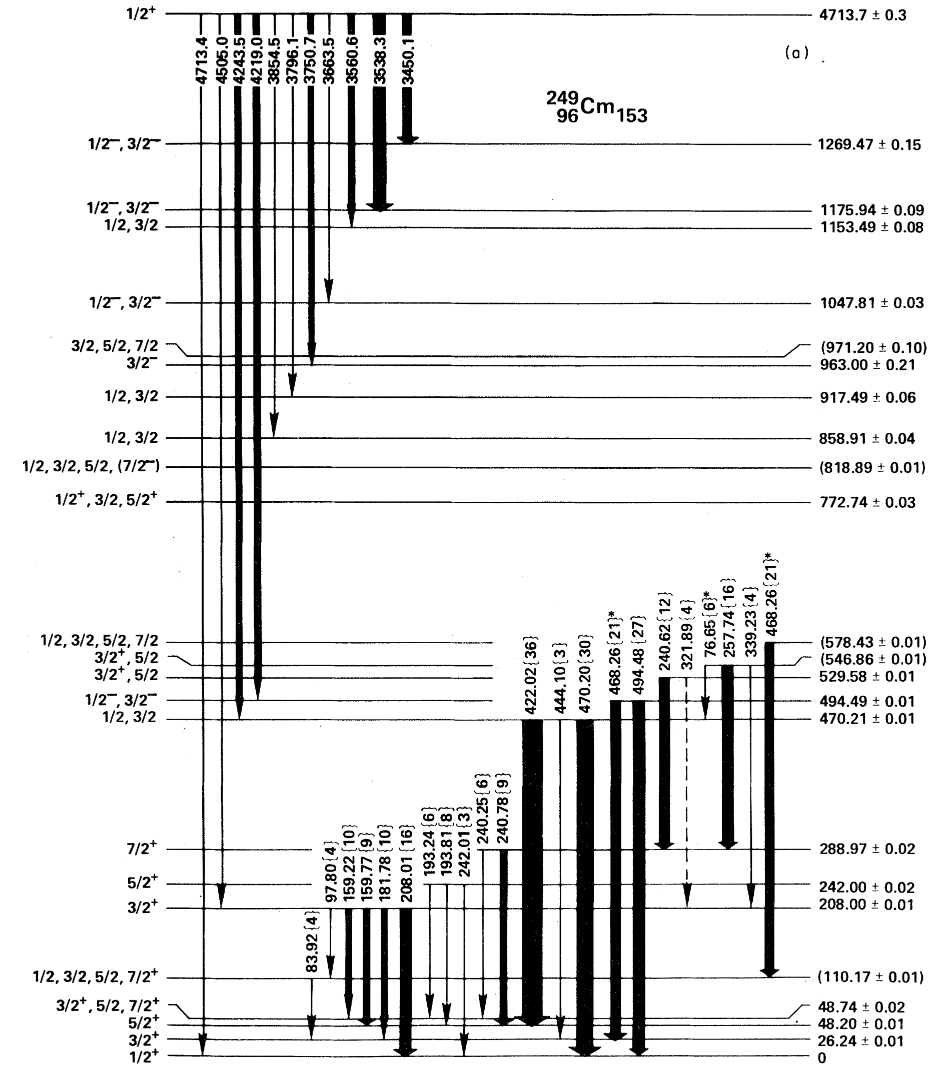

FIG. 1. Level scheme of ^{249}Cm based upon model-independent evidence and including gamma-ray transition energies (keV) and intensities (photons per 1000 captures). Levels whose energies are given in parentheses were derived from evidence which includes some model-dependent arguments. An asterisk denotes multiple placement of a transition. (a) Primary transitions and secondary transitions for levels below 600 keV. (b) Secondary transitions for levels above 600 keV.

Levels at 470.21 and 494.49 keV. There are relatively strong primary transitions that feed these levels; the intensity of the primary gamma feeding the 494 keV level is considered large enough to limit spin and parity assignments to $\frac{1}{2}^-$ or $\frac{3}{2}^-$. A level at 469$\pm$2 keV is indicated by the (d,p) reaction spectroscopy. The 470 keV level deexcites to the $\frac{1}{2}$, $\frac{3}{2}$, and $\frac{5}{2}$ members of the ground state band. The 494 keV level deexcites to the $\frac{1}{2}$ and $\frac{3}{2}$ members of the ground state band. Spin and parity assignments for these levels are $\frac{1}{2}$, $\frac{3}{2}$ (470.21 keV) and $\frac{1}{2}^-$, $\frac{3}{2}^-$ (494.49 keV).

Level at 529.58 keV. A level at 528$\pm$3 keV was observed in the (d,p) measurement. We observe two gamma rays that deexcite this level and one that feeds it from above. Allowable spin and parity assignments are $\frac{3}{2}^+$ and $\frac{5}{2}$.

Level at 546.86 keV. The evidence for this level is considered tentative; we observe two gamma rays deexciting the level to the 208 and 289 keV levels of a lower band and four gamma rays feeding the level from above. Allowable spin and parity assignments are $\frac{3}{2}^+$ and $\frac{5}{2}$.

Level at 578.43 keV. Based on model-dependent

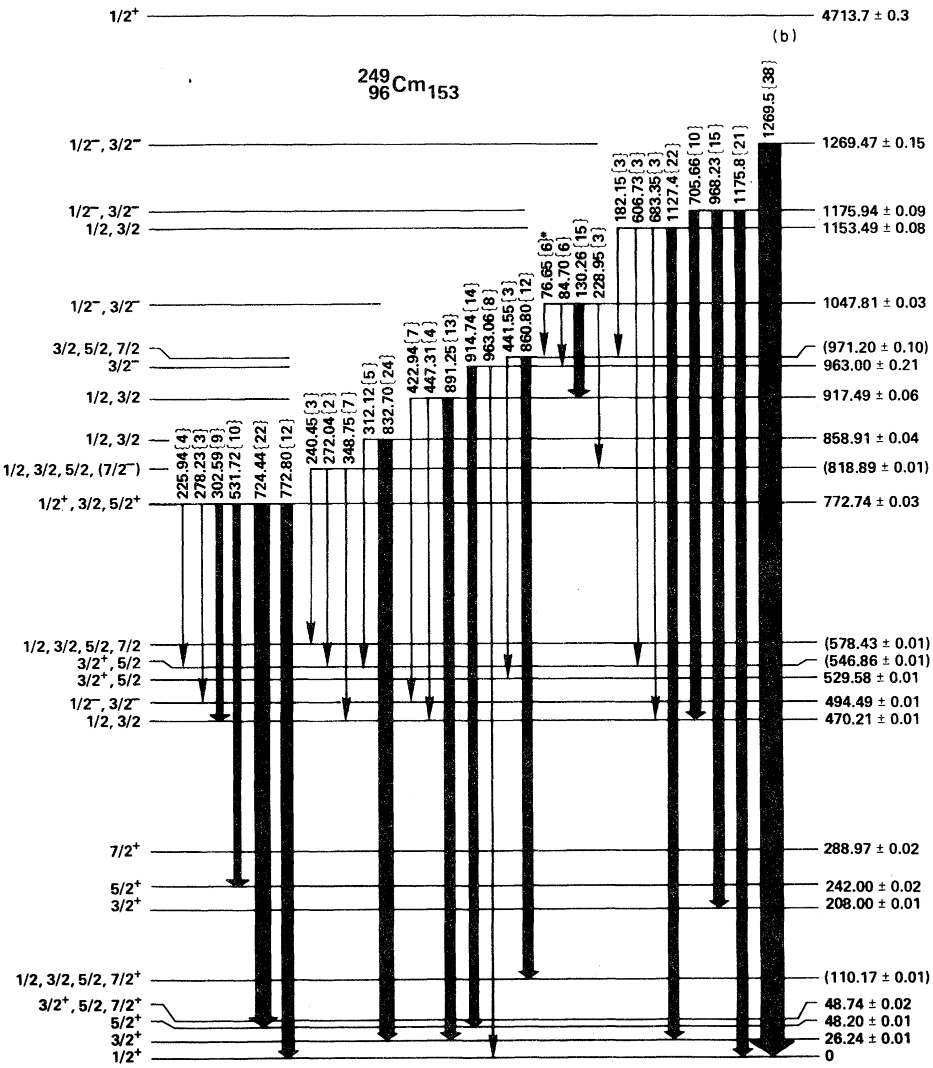

FIG. 1. (*Continued.*)

arguments presented later in this paper, an $I=\frac{7}{2}$ level is expected to exist at approximately 576 keV. This estimated level energy is derived from an observed level spacing for the $I=\frac{5}{2}$ and $\frac{9}{2}$ members of the rotational band. The $I=\frac{7}{2}$ member is tentatively assigned at 578.43 keV based upon a depopulating gamma ray to the 110.17-keV level and feeding by a gamma ray from an 818.89-keV level.

Level at 772.74 keV. Although we do not observe a primary transition to this level, there is good evidence for its existence in that we observe six gamma rays that depopulate it. Allowable spin and parity assignments for the level are $\frac{1}{2}^+$, $\frac{3}{2}$, and $\frac{5}{2}^+$.

Level at 818.89 keV. In a later section of this paper that includes model-dependent arguments, we propose the existence of a $K=\frac{3}{2}$ band (configuration: $\frac{3}{2}^-$ [752]) based at 772 keV. The expected energy for the $I=\frac{5}{2}$ level of this band, which is derived in a calculation that includes Coriolis mixing, is approximately 820 keV. Based upon three deexciting gamma rays, we establish the existence of this level at 818.89±0.02 keV.

Levels at 858.91, 917.49, and 963.00 keV. Each of these levels is populated by a primary transition. Therefore, the spin assignments can be limited to $\frac{1}{2}$, $\frac{3}{2}$, and $\frac{5}{2}^+$. Given the relatively low sensitivity of our primary transition measurements, we can rule out population of $\frac{5}{2}^+$ states. For the 858 and 917 keV levels, allowable spin and parity assignments are $\frac{1}{2}$ and $\frac{3}{2}$. For the 963 keV level, the reduced primary transition intensity is large enough that allowable spin and parity assignments for this level are $\frac{1}{2}^-$ and $\frac{3}{2}^-$. We also observe secondary gamma rays from each level that feed into the well-established level structure below 550 keV. Since the 963 keV level decays to a $\frac{5}{2}^+$ level at 48.2 keV, its spin and parity assignments are uniquely determined to be $\frac{3}{2}^-$.

Level at 971.20 keV. In a later section of this paper, we assign the 917- and 963-keV levels as the first two members of a $K=\frac{1}{2}$ band (configuration: $\frac{1}{2}^-$[501]). We propose the existence of a third level in this band at 971.20±0.10 keV based upon two deexciting gamma rays.

Levels at 1047.81 keV. A moderately intense primary transition indicates the presence of a level at 1049.9±0.2 keV. Four secondary gamma rays can be combined in a Ritz combination to define a level at 1047.81±0.03 keV. The energy of each depopulating transition corresponds to the indicated level spacing within one standard deviation. The total intensity carried away by the depopulating transitions (31 relative units, photons per 1000 captures) is consistent with feeding by a moderately intense primary. In a later section of this paper, we assign three of the populated levels to the $I=\frac{1}{2}$, $\frac{3}{2}$, and $\frac{5}{2}$ members of the $\frac{1}{2}^-$[501] orbital. Thus, the experimental evidence for the existence of a 1047.81 keV level is quite convincing. On the other hand, the difference between the level energy defined by the depopulating transitions and that defined by the primary transition is more than 2 keV which is a much larger discrepancy than observed for any of the other levels and which is four times larger than the propagated error. Since Ritz combinations do not offer any other attractive possibilities for a level with energy closer to 1049.9 keV and with sufficient intensity for the depopulating transitions, we assign a level at 1047.81±0.03 keV, although it is questionable whether the level populated by the primary transition and the assigned level are identical.

Levels at 1153.49, 1175.94, and 1269.47 keV. Each of these levels is populated by a strong primary transition. The transition to the 1153.49 keV level is partially obscured by an *A*1 capture line which results in a large uncertainty on the intensity. We assign allowable spin and parity values to this level of $\frac{1}{2}^{\pm}$ and $\frac{3}{2}^{\pm}$. The two higher levels are assigned $\frac{1}{2}^-$ and $\frac{3}{2}^-$ on the basis of the primary line intensities.

B. Application of the Nilsson model to the level scheme

Since the actinide species constitute a region of nuclei that exhibit stable quadrupole deformation in their ground states, one can use the "unified" model of Bohr and Mottelson[15] to predict a variety of properties for excited nuclear levels. This model combines features of the nuclear shell model with a description of collective excitation, both rotational and vibrational. For odd-mass nuclei, a basic assumption is that the unpaired nucleon is considered to move according to an average potential generated by the combined effect of all of the remaining (paired) nucleons. Corrections are added for perturbations due to nuclear pairing effects. An early development of these ideas was that of Nilsson and co-workers[16] who employed a harmonic oscillator potential, a spin-orbit coupling term, and an l^2 term in their Hamiltonian to solve this problem. Since its original formulation, this oscillator potential has been modified, chiefly in the treatment of the l^2 term so that the spacing between adjacent oscillator shells remains exactly $\hbar\omega_0$, and in the introduction of a deformation dependence in the spin-orbit and l^2 terms. In addition, extensive calculations have been made using the more realistic Woods-Saxon potential.[17] Chasman *et al.*[1] present a good discussion of the detail and merits of these potential forms. The harmonic oscillator potential is attractive due to the relative ease of calculation. Chasman *et al.*[1] have reviewed the experimental evidence and find that wave functions obtained from the Woods-Saxon potential agree better with experimental data than those obtained from the modified oscillator potential.

We have chosen to calculate eigenvalues and wave functions for single-particle configurations of ^{249}Cm with the modified oscillator potential; we employed a computer code CJ written by Nilsson.[18] For values of the parameters that describe the potential, we have adopted $\kappa=0.0635$ and $\mu=0.317$, as recommended for $A=249$ by Nilsson *et al.*,[19] who derived these values by making the best fit to experimental level energies of nuclei near $A=242$.

Another set of parameters required for these calculations are those describing the deformation of the nucleus. Ground-state equilibrium distortion can be calculated for a given nucleus by minimizing the potential energy with respect to the deformation parameters ϵ_2 and ϵ_4. The potential energy is calculated using the liquid drop model with shell corrections. Many calculations of distortion parameters for actinides have been done over the years; recent results using both modified oscillator and Woods-Saxon potentials are in good agreement. We list the results of Møller *et al.*[20] in footnote a of Table IV; these values were derived by interpolating between

TABLE V. Experimental and calculated excited levels for ^{249}Cm.

	Experimental		MO calculations[a]		Calculations of Gareev *et al.*[b]			Woods-Saxon potential[d]
Configuration	Energy (keV)	Decoupling parameter	Energy (keV)	Decoupling parameter	Energy (keV)	Percentage indicated configuration	Other important configurations[c]	Decoupling parameter
$\frac{1}{2}^{+}$[620]	0	+0.33	0	−0.91	0	81%		+0.29
$\frac{7}{2}^{+}$[613]	48.7		65		70	83%		
$\frac{3}{2}^{+}$[622]	208.0		60		150	72%		
$\frac{11}{2}^{-}$[725]			−85		430	85%		
$\frac{1}{2}^{-}$[761]	470.2	−1.89	460	−5.0	500	52%	$622+Q_1(31)$ 11%	−3.36
							$620+Q_1(30)$ 10%	
$\frac{9}{2}^{-}$[734]			440		510	86%		
$\frac{5}{2}^{+}$[622]	529.6		1260		900	56%	$734+Q_1(32)$ 20%	
$\frac{3}{2}^{-}$[752]	772.7		1150		910	37%	$620+Q_1(31)$ 29%	
							$622+Q_1(30)$ 18%	
$\frac{1}{2}^{-}$[501]	917.5	+0.80	2520	+1.0	920	65%	$752+Q_1(22)$ 19%	+0.76
							$761+Q_1(22)$ 12%	
$\frac{1}{2}^{+}$[631]			1360	−0.04	1200	80%		−0.70
$\frac{1}{2}^{-}$[750]			2000	+5.5				

[a]Modified oscillator potential: $\kappa=0.0635$, $\mu=0.317$. For ^{249}Cm, $\epsilon_2=0.22$, and $\epsilon_4=0$. Calculations performed with CJ code.
[b]Reference 23, Woods-Saxon potential plus quasiparticle-phonon interaction. For ^{249}Cm, $\epsilon_2=0.25$ and $\epsilon_4=-0.003$.
[c]Notation is that of Ref. 23.
[d]Chasman *et al.*, Ref. 1, calculation with $\epsilon_2=0.239$, $\epsilon_4=0$, $A=244$.

calculated results for the nuclei ^{248}Cm and ^{250}Cm.

The results of our calculations for single-particle excitations in ^{249}Cm are listed in Table V. The energies listed are those for the bandhead levels. The theoretical quasiparticle energy is given by the expression

$$E_{\mathrm{qp}}^{\nu}=\sqrt{(E_{\mathrm{sp}}^{\nu}-\lambda)^2+\Delta^2}\ ,$$

where the parameters are λ, the Fermi level, and Δ, the pairing gap. For this latter quantity, we have used an approximation that the pair gap parameter is equal to the odd-even mass difference,

$$\Delta M_{0e}=M(^{249}\mathrm{Cm})-[\tfrac{3}{8}M(^{250}\mathrm{Cm})+\tfrac{3}{4}M(^{248}\mathrm{Cm}) - \tfrac{1}{8}M(^{246}\mathrm{Cm})]=664\ \mathrm{keV}\ .$$

This formula was given by Mang *et al.*[21] and the masses were taken from a compilation by Wapstra and Bos.[22] As shown in Table V, three other configurations lie close in energy to the ground state configuration, namely $\frac{7}{2}^{+}$[613], $\frac{3}{2}^{+}$[622], and $\frac{11}{2}^{-}$[725]. For this calculation we have simply assumed $\lambda=E_{\mathrm{sp}}$ for the $\frac{1}{2}^{+}$ [620] configuration. Adjustment of the assumed value of the Fermi level will cause these low-lying configurations to shift in energy, but these variations do not substantially improve our understanding of, or agreement with, the experimental results.

For comparison, we have listed in Table V the predicted bandhead energies for ^{249}Cm according to the calculations of Gareev *et al.*[23] who employed a Woods-Saxon potential and included quasiparticle-phonon interactions. When there are significant admixtures of vibrational components in a given configuration, we have indicated these admixtures in column 8 of the table, using their original notation. The calculated level energies listed in the table show reasonable agreement except for two configurations, $\frac{11}{2}^{-}$[725] and $\frac{1}{2}^{-}$[501]. We do not have experimental evidence for existence of the first configuration. In the latter case, apparently we can expect the energy of this $\frac{1}{2}^{-}$[501] configuration to be significantly lowered due to quasiparticle-phonon interactions. Two other configurations, $\frac{1}{2}^{-}$[761] and

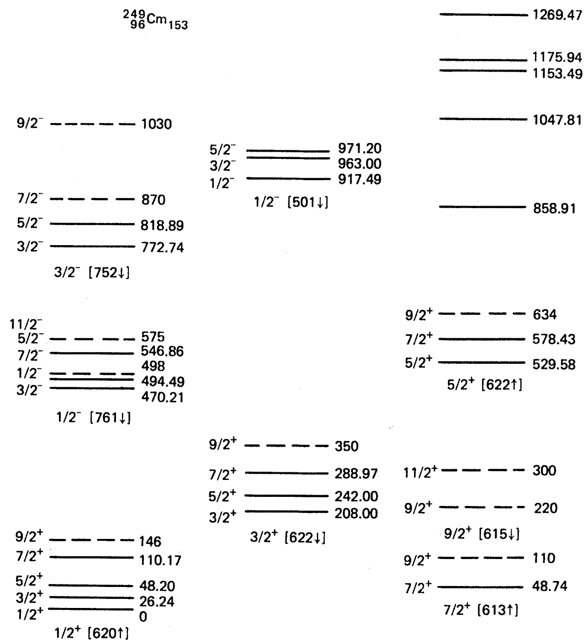

FIG. 2. Level scheme of ^{249}Cm showing rotational bands and configuration assignments from the Nilsson model. Levels observed in the ^{248}Cm$(d,p)^{249}$Cm reaction (Ref. 3), but not populated in the (n,γ) reaction are indicated as dashed lines. Some unassigned levels are given in the right side of the figure.

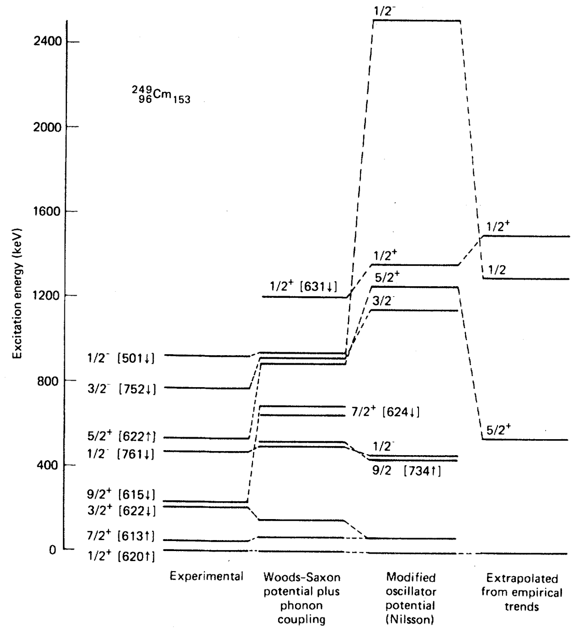

FIG. 3. ^{249}Cm bandhead energies, experimental vs theoretical. The experimental bandhead energies with their associated configuration assignments are compared with theoretical excitation energies from (1) Soloviev's group who assumed a Woods-Saxon potential form and included quasiparticle-phonon coupling, (2) a modified oscillator potential calculation done with the *CJ* code, $\kappa=0.0635$ and $\mu=0.317$, and (3) extrapolation of empirical trends in neighboring nuclei.

$\frac{3}{2}^-[752]$, are calculated to include important vibrational components; the indicated single-particle configurations comprise only 52% and 37%, respectively, of the total wave function.

Calculated decoupling parameters are listed for the $\Omega=\frac{1}{2}$ bands in Table V, based upon both a modified oscillator (mo) potential calculation and a Woods-Saxon potential calculation. Comparison of the results from the calculations shows some large differences. For the $\frac{1}{2}^+[620]$ configuration, the mo calculation predicts $a=-0.91$, while the Woods-Saxon calculation predicts $a=+0.29$. A summary of experimental values for this configuration, as reported by Chasman *et al.*,[1] shows much better agreement with the Woods-Saxon calculations. They find similar agreement between experiment and theory (Woods-Saxon potential) for the $\frac{1}{2}^+[631]$ configuration in a number of nuclei. Faessler and Sheline[24] have made a comparison between wave functions calculated using a Woods-Saxon potential and a harmonic oscillator potential in the rare-earth region; they find that experimental values for the decoupling parameter of a $\frac{1}{2}^-[510]$ band are reproduced more accurately in the Woods-Saxon calculations. On this basis, the decoupling parameters in the last column of Table V are considered the preferred calculated values in examination of our results for ^{249}Cm.

Guided by the nuclear model predictions for single-particle states in ^{249}Cm and making use of our model-independent level scheme, we proceed to the identification of rotational bands and the assignment of Nilsson configurations. The regularity of rotational bands is expressed in the well-known formula

$$E_I=E_0+\hbar^2/2J[I(I+1)+\delta_{K,1/2}(-1)^{I+1/2}(I+1/2)a]\ .$$

For some of the less perturbed configurations in odd-mass actinide elements, rotational parameters of $\hbar^2/2J\equiv A=6.2-6.6$ are observed experimentally.

One may derive empirical values of A from experimental data that sometimes show large deviations from the indicated range of unperturbed bands. Usually, these observations can be explained by the presence of significant Coriolis mixing. This

TABLE VI. Summary of experimental energies and Nilsson-model configuration assignments for ^{249}Cm levels.

Best experimental level energy (keV)	Primary transition data: Level energy (keV)	Reaction spectroscopy data[a]: Level energy (keV)	Model independent spin, parity	Nilsson-model spin, parity, and configuration
0	0	0	$\frac{1}{2}+$	$\frac{1}{2}+\ \frac{1}{2}[620]$
26.24±0.01	b	25±2	$\frac{3}{2}+$	$\frac{3}{2}+\ \frac{1}{2}[620]$
48.20±0.01		48±1	$\frac{5}{2}+$	$\frac{5}{2}+\ \frac{1}{2}[620]$
110.17±0.01		110±1	$\frac{1}{2},\frac{3}{2},\ \frac{5}{2},\frac{7}{2}+$	$\frac{7}{2}+\ \frac{1}{2}[620]$
48.74±0.02			$\frac{3}{2}+,\frac{5}{2},\frac{7}{2}+$	$\frac{7}{2}+\ \frac{7}{2}[613]$
110 ±1		110±1		$\frac{9}{2}+\ \frac{7}{2}[613]$
208.00±0.01	208.4±0.5	208±1	$\frac{3}{2}+$	$\frac{3}{2}+\ \frac{3}{2}[622]$
242.00±0.02		242±1	$\frac{5}{2}+$	$\frac{5}{2}+\ \frac{3}{2}[622]$
288.97±0.02		288±5	$\frac{7}{2}+$	$\frac{7}{2}+\ \frac{3}{2}[622]$
350 ±1		350±1		$\frac{9}{2}+\ \frac{3}{2}[622]$
470.21±0.01	469.9±0.5	469±2	$\frac{3}{2}-$	$\frac{3}{2}-\ \frac{1}{2}[761]$
494.49±0.01	494.4±0.5		$\frac{1}{2}-,\frac{3}{2}-$	$\frac{1}{2}-\ \frac{1}{2}[761]$
498 ±3		498±3		$\frac{7}{2}-\ \frac{1}{2}[761]$
546.86±0.01			$\frac{3}{2}+,\frac{5}{2}$	$\frac{5}{2}-\ \frac{1}{2}[761]$
575 ±3		575±3		$\frac{11}{2}-\ \frac{1}{2}[761]$
529.58±0.01		528±3	$\frac{3}{2}+,\frac{5}{2}$	$\frac{5}{2}+\ \frac{5}{2}[622]$

effect is most important for configurations with a high j quantum number in the spherical state; thus, in ^{249}Cm we expect considerable mixing among the $h_{11/2}$ set of configurations, in particular, $\frac{1}{2}^-[761]$ and $\frac{3}{2}^-[752]$.

In this model-dependent derivation of the ^{249}Cm level scheme, we also employ the data of BCEF whose measurements provide level energies and cross sections for (d,p) population of certain members of rotational bands where the configurations have a significant amount of particle character. BCEF list data for the (d,p) spectrum up to a level energy of 1650 keV. The uncertainties on level energies are in the range of 1–7 keV. They provided interpretation for only the lower portion of the spectrum, in the energy range 0–575 keV.

Another set of experimental results, useful in the interpretation of our experiment, is that for the level scheme of ^{251}Cf ($N=153$) where the information was derived mainly from a study of the ^{255}Fm α spectrum and the photons following this α decay.[25] In this work, the following single particle configurations (followed by a bandhead energy) were assigned: $\frac{1}{2}^+[620]$, 0 keV; $\frac{7}{2}^+[613]$, 106 keV; $\frac{3}{2}^+[622]$, 178 keV; $\frac{11}{2}^-[725]$, 370 keV; $\frac{9}{2}^-[734]$, 434 keV; and $\frac{5}{2}^+[622]$, 544 keV.

In the following paragraphs, we discuss evidence for each configuration assignment. These experimental data and the configuration assignments are summarized in Table VI and Figs. 2 and 3.

$\frac{1}{2}^+[620]$. The ground state rotational band for ^{249}Cm has been assigned the configuration $\frac{1}{2}^+[620]$.[3,10] From our level energy measurements,

TABLE VI. (*Continued.*)

Best experimental level energy (keV)	Primary transition data: Level energy (keV)	Reaction spectroscopy data[a]: Level energy (keV)	Model independent spin, parity	Nilsson-model spin, parity, and configuration
578.43±0.01			$\frac{1}{2},\frac{3}{2},\frac{5}{2},\frac{7}{2}$	$\frac{7}{2}^{+}$ $\frac{5}{2}$[622]
634 ±2		634±2		$\frac{9}{2}^{+}$ $\frac{5}{2}$[622]
772.74±0.03			$\frac{1}{2}^{+},\frac{3}{2},\frac{5}{2}^{+}$	$\frac{3}{2}^{-}$ $\frac{3}{2}$[752]
818.89±0.01			$\frac{1}{2},\frac{3}{2},\frac{5}{2},\frac{7}{2}^{-}$	$\frac{5}{2}^{-}$ $\frac{3}{2}$[752]
870 ±4		870±4		$\frac{7}{2}^{-}$ $\frac{3}{2}$[752]
1030 ±7		1030±7		$\frac{11}{2}^{-}$ $\frac{3}{2}$[752]
858.91±0.04	858.8±0.9		$\frac{1}{2},\frac{3}{2}$	
917.49±0.06	917.3±0.5	(915±2)[c]	$\frac{1}{2}^{-},\frac{3}{2}^{-}$ $\frac{1}{2}^{-}$	$\frac{1}{2}$[501]
963.00±0.21	962.7±0.5		$\frac{3}{2}^{-}$	$\frac{3}{2}^{-}$ $\frac{1}{2}$[501]
971.20±0.10			$\frac{3}{2},\frac{5}{2},\frac{7}{2}$	$\frac{5}{2}^{-}$ $\frac{1}{2}$[501]
1047.81±0.03	1049.9±0.5		$\frac{1}{2}^{-},\frac{3}{2}^{-}$	
1153.49±0.08	1152.8±1.1		$\frac{1}{2},\frac{3}{2}$	
1175.94±0.09	1175.0±0.5		$\frac{1}{2}^{-},\frac{3}{2}^{-}$	
1269.47±0.15	1268.5±0.5		$\frac{1}{2}^{-},\frac{3}{2}^{-}$	

[a]Data of Ref. 3.
[b]Possible primary transition obscured by intense Al line.
[c]This peak in the (*d,p*) spectrum is not assigned to the $\frac{1}{2}$[501] configuration.

TABLE VII. Gamma ray transitions depopulating ^{249}Cm levels.

Level energy (keV)	Spin, parity, configuration	Depopulating gamma ray transitions: Gamma energy (keV)	Experimental reduced transition rate[a]	Theoretical reduced transition rate[b]	Populated level (keV)	Spin, parity	Configuration[c]	Remarks
0	$\frac{1}{2}^{+}\frac{1}{2}$[620]							
26.24	$\frac{3}{2}^{+}\frac{1}{2}$[620]							
48.20	$\frac{5}{2}^{+}\frac{1}{2}$[620]							
110.17	$\frac{7}{2}^{+}\frac{1}{2}$[620]	83.92			26.2	$\frac{3}{2}^{+}$	$\frac{1}{2}$[620]	*E*2
48.74	$\frac{7}{2}^{+}\frac{7}{2}$[613]							

TABLE VII. (*Continued.*)

Level energy (keV)	Spin, parity, configuration	Depopulating gamma ray transitions: Gamma energy (keV)	Experimental reduced transition rate[a]	Theoretical reduced transition rate[b]	Populated level (keV)	Spin, parity	Configuration[c]	Remarks
110	$\frac{9}{2}^+\frac{7}{2}[613]$							
208.00	$\frac{3}{2}^+\frac{3}{2}[622]$	208.01	0.79	1.28	0	$\frac{1}{2}^+$	$\frac{1}{2}[620]$	
		181.78	0.77	1.02	26.2	$\frac{3}{2}^+$		
		159.77	1.00	0.26	48.2	$\frac{5}{2}^+$		
		159.22			48.7	$\frac{7}{2}^+$	$\frac{7}{2}[613]$	$E2$
		97.80			110.2	$\frac{7}{2}^+$	$\frac{1}{2}[620]$	$E2$
242.00	$\frac{5}{2}^+\frac{3}{2}[622]$	242.01	0.18		0	$\frac{1}{2}^+$	$\frac{1}{2}[620]$	$E2$
		193.81	1.00		48.2	$\frac{5}{2}^+$		
		193.24	0.69		48.7	$\frac{7}{2}^+$	$\frac{7}{2}[613]$	d
288.97	$\frac{7}{2}^+\frac{3}{2}[622]$	240.78	1.00		48.2	$\frac{5}{2}^+$	$\frac{1}{2}[620]$	
		240.25	0.64		48.7	$\frac{7}{2}^+$	$\frac{7}{2}[613]$	d
350	$\frac{9}{2}^+\frac{3}{2}[622]$							
470.21	$\frac{3}{2}^-\frac{1}{2}[761]$	470.20	0.60		0	$\frac{1}{2}^+$	$\frac{1}{2}[620]$	
		444.10	0.06		26.2	$\frac{3}{2}^+$		
		422.02	1.00		48.2	$\frac{5}{2}^+$		
494.49	$\frac{1}{2}^-\frac{1}{2}[761]$	494.48	1.00		0	$\frac{1}{2}^+$	$\frac{1}{2}[620]$	
		468.26[e]	0.90		26.2	$\frac{3}{2}^+$		
498	$\frac{7}{2}^-\frac{1}{2}[761]$							
546.86	$\frac{5}{2}^-\frac{1}{2}[761]$	339.23	0.008	0.009	208.0	$\frac{3}{2}^+$	$\frac{3}{2}[622]$	
		257.74	0.067	0.066	289.0	$\frac{7}{2}^+$		
		76.65[e]	1.000		470.2	$\frac{3}{2}^-$	$\frac{1}{2}[761]$	
575	$\frac{11}{2}^-\frac{1}{2}[761]$							
529.58	$\frac{5}{2}^+\frac{5}{2}[622]$	321.89	0.13	1.05	108.0	$\frac{3}{2}^+$	$\frac{3}{2}[622]$	
		240.62	1.00	0.08	289.0	$\frac{7}{2}^+$		
578.43	$\frac{7}{2}^+\frac{5}{2}[622]$	468.26[e]			110.2	$\frac{7}{2}^+$	$\frac{1}{2}[620]$	d
634	$\frac{9}{2}^+\frac{5}{2}[622]$							
772.74	$\frac{3}{2}^-\frac{3}{2}[752]$	772.80	0.07	0.04	0	$\frac{1}{2}^+$	$\frac{1}{2}[620]$	
		724.44	0.16	0.19	48.2	$\frac{5}{2}^+$		
		531.72	0.18		242.0	$\frac{5}{2}^+$	$\frac{3}{2}[622]$	
		302.59	0.84	0.90	470.2	$\frac{3}{2}^-$	$\frac{1}{2}[761]$	
		278.23	0.41	1.12	494.5	$\frac{1}{2}^-$		
		225.94	1.00	0.23	546.9	$\frac{5}{2}^-$		
818.89	$\frac{5}{2}^-\frac{3}{2}[752]$	348.75	0.79	0.61	470.2	$\frac{3}{2}^-$	$\frac{1}{2}[761]$	
		272.04	0.51	0.69	546.9	$\frac{5}{2}^-$		
		240.45	1.00		578.4	$\frac{7}{2}^+$	$\frac{5}{2}[622]$	

TABLE VII. (*Continued.*)

		Depopulating gamma ray transitions						
Level energy (keV)	Spin, parity, configuration	Gamma energy (keV)	Experimental reduced transition rate[a]	Theoretical reduced transition rate[b]	Populated level (keV)	Spin, parity	Configuration[c]	Remarks
870	$\frac{7}{2}^{-}\frac{3}{2}[752]$							
1030	$\frac{11}{2}^{-}\frac{3}{2}[752]$							
858.91	$(\frac{1}{2},\frac{3}{2})$	832.70	0.24		26.2	$\frac{3}{2}^{+}$	$\frac{1}{2}[620]$	
		312.12	1.00		546.9	$\frac{5}{2}^{-}$	$\frac{1}{2}[761]$	
917.49	$\frac{1}{2}^{-}\frac{1}{2}[501]$	891.25	0.18		26.2	$\frac{3}{2}^{+}$	$\frac{1}{2}[620]$	
		447.31	0.50		470.2	$\frac{3}{2}^{-}$	$\frac{1}{2}[761]$	
		422.94	1.00		494.5	$\frac{1}{2}^{-}$		
963.00	$\frac{3}{2}^{-}\frac{1}{2}[501]$	963.06	0.54		0	$\frac{1}{2}^{+}$	$\frac{1}{2}[620]$	
		914.74	1.96		48.2	$\frac{5}{2}^{+}$		
971.20	$\frac{5}{2}^{-}\frac{1}{2}[501]$	860.80	0.60		110.2	$\frac{7}{2}^{+}$	$\frac{1}{2}[620]$	
		441.55	1.00		529.6	$\frac{5}{2}^{+}$	$\frac{5}{2}[622]$	f
1047.81	$(\frac{1}{2}^{-},\frac{3}{2}^{-})$	228.95	0.02		818.9	$\frac{5}{2}^{-}$	$\frac{3}{2}[752]$	
		130.26	0.50		917.5	$\frac{1}{2}^{-}$	$\frac{1}{2}[501]$	
		84.70	0.75		963.0	$\frac{3}{2}^{-}$		
		76.65[e]	1.00		971.2	$\frac{5}{2}^{-}$		
1153.49	$(\frac{1}{2},\frac{3}{2})$	1127.4	0.031		26.2	$\frac{3}{2}^{+}$	$\frac{1}{2}[620]$	
		683.35	0.019		470.2	$\frac{3}{2}^{-}$	$\frac{1}{2}[761]$	
		606.73	0.027		546.9	$\frac{5}{2}^{-}$		
		182.15	1.000		971.2	$\frac{5}{2}^{-}$	$\frac{1}{2}[501]$	
1175.94	$(\frac{1}{2}^{-},\frac{3}{2}^{-})$	1175.8	0.44		0	$\frac{1}{2}^{+}$	$\frac{1}{2}[620]$	
		968.23	0.58		208.0	$\frac{3}{2}^{+}$	$\frac{3}{2}[622]$	
		705.66	1.00		470.2	$\frac{3}{2}^{-}$	$\frac{1}{2}[761]$	
1269.47	$(\frac{1}{2}^{-},\frac{3}{2}^{-})$	1269.5			0	$\frac{1}{2}^{+}$	$\frac{1}{2}[620]$	

[a]Reduced transition rates have been calculated assuming each transition is of either pure $M1$ or pure $E1$ character. Transitions assigned $E2$ character are not included in this calculation. These relative rates are normalized to the most rapid transition (=1.00).
[b]Theoretical rates are given for dipole transitions between pure single particle configurations. These relative rates are normalized such that the total theoretical transition strength is equal to the total experimental transition strength for population of a given rotational band; the units, which are relative, are taken from the adjacent column of experimental data.
[c]If a configuration is not shown, the level has the same configuration as the nearest labeled level above.
[d]M1 transition is K forbidden; $E2$ transition is allowed.
[e]Transition placed twice in level scheme.
[f]$E1$ transition is K forbidden by one unit.

we extract values of $A(\equiv\hbar^2/2\mathcal{J})=6.572\pm0.002$ keV and $a=+0.330\pm0.001$. We calculate level energies of 109.4 and 149.0 keV for the $I=\frac{7}{2}$ and $\frac{9}{2}$ levels in this band; the level observed at 110.17 keV in this experiment and the (d,p) level energies of 110 ± 1 and 146 ± 3 keV show satisfactory agreement with these calculated values. Our rotational parameters are close to those obtained for the same configuration in ^{251}Cf, $A = 6.438 \pm 0.002$ keV and $a = +0.285 \pm 0.001$. Our experimental value for the decoupling parameter, $a = +0.330$, is in reasonable agreement with the preferred calculated value, $a = +0.29$.

$\frac{7}{2}^+$[613]. In interpreting the ^{248}Cm(*d,p*) spectrum, BCEF assigned a prominent peak, corresponding to a level at 110 ± 1 keV, to the $I = \frac{9}{2}$ member of a $\frac{7}{2}^+$[613] rotational band. Although it was recognized that the $I = \frac{7}{2}$, $\frac{1}{2}^+$[620] level occurs at 110 keV, BCEF made this assignment to the $\frac{7}{2}^+$[613] configuration in order to explain the intensity of the observed peak. The $\frac{7}{2}^+$[613] configuration is expected to be populated in the favored alpha decay of ^{253}Cf, also. Bemis and Halperin[4] have observed just two α groups for ^{253}Cf decay, at 5.979 MeV (94.7%) and 5.921 MeV (5.3%). Both groups exhibit low hindrance factors which are indicative of favored decay. Since their experiment did not provide information on the absolute energy of the levels being populated, Bemis and Halperin[4] adopted the BCEF assignment, i.e., they assumed the higher energy alpha group populates a level at 110 keV. The foregoing information suggests the $\frac{7}{2}^+$[613] bandhead occurs at about 52 keV.

We find evidence for a level at 48.74 ± 0.01 keV with possible spin and parity assignments of $\frac{3}{2}^+$, $\frac{5}{2}$,

TABLE VIII. Results of Coriolis mixing calculation for $N = 7$ configurations in ^{249}Cm.

	Level energies (keV)			Cross section in μb/sr for ^{248}Cm (*d,p*) at 140° $d\sigma/d\Omega_{calc}$		
I	E_{calc}	E_{exp}	ΔE	mixing	no mixing	$d\sigma/d\Omega_{exp}$[a]
		$\frac{1}{2}$[761]				
$\frac{1}{2}$	494.9	494.49(1)	+0.5	22	22	
$\frac{3}{2}$	468.7	470.21(1)	−1.5	82	93	138±28
$\frac{5}{2}$	547.1	546.86(1)	+0.2	17	25	70±23
$\frac{7}{2}$	498.4	498(3)	+0.4	92	150	240±48
$\frac{9}{2}$	630.8			5	10	
$\frac{11}{2}$	575.5	575(3)	+0.5	21	50	80±25
$\frac{13}{2}$	755.2			0.7	1.3	
$\frac{15}{2}$	704.0			0.9	0.2	
		$\frac{3}{2}$[752]				
$\frac{3}{2}$	770.2	772.74(4)	−2.5	31	16	
$\frac{5}{2}$	820.5	818.89(2)	+1.6	30	17	
$\frac{7}{2}$	871.6	870(4)	+1.6	149	93	60±20
$\frac{9}{2}$	968.8			27	20	
$\frac{11}{2}$	1030.6	1030(7)	−0.6	61	52	160±40
$\frac{13}{2}$	1174.5			5	4	
$\frac{15}{2}$	1238.8			2	2	

Parameters derived from calculation	Theoretical	Fit to experiment	Reduction factor
$h^2/2J$		6.41	
$a, \frac{1}{2}$[761]	−3.36	−1.89	0.56
$\langle K \mid j_- \mid K' \rangle \frac{1}{2}[761] - \frac{3}{2}[752]$	+5.1	+4.4	0.86

[a]These data are taken from Ref. 3.

and $\frac{7}{2}^+$. We assign the $\frac{7}{2}^+$[613] configuration to the 48.74 keV level. This configuration is known to occur at 106 keV in ^{251}Cf. The $\frac{7}{2}$-$\frac{9}{2}$ level spacing in ^{251}Cf, 60.0 keV, agrees with the observed spacing of 61 keV in ^{249}Cm. The gamma transitions observed to feed the 48.74 keV level from the 208, 242, and 289 keV levels are K forbidden in terms of $M1$ multipolarity, on the basis of our configuration assignment.

$\frac{3}{2}^+$[622]. This configuration was assigned by BCEF to a rotational band consisting of four levels beginning at 208 keV. We observe the three lowest levels and have adopted the spin, parity, and configuration assignments of BCEF in the construction of our level scheme. We calculate an average rotational parameter, $A=6.76\pm0.05$ keV, which is identical to that observed for the same configuration in ^{251}Cf, $A=6.75\pm0.07$ keV. Deexcitation of the 208 and 242 keV levels to members of the ground state bands is examined in Table VII where we compare experimental data with predicted relative reduced transition probabilities given by Clebsch-Gordan coefficients, assuming the transitions to be pure $M1$. For the 242 keV level, relative rates from experiment agree well with theory; for the 208 keV level, agreement is less satisfactory.

$\frac{5}{2}^+$[622]. This configuration is known to exist in ^{251}Cf with the bandhead at 544 keV. There is evidence for its existence in the lighter odd-mass Cm isotopes where the $I=\frac{5}{2}$ and $\frac{9}{2}$ members are identified in (d,p) spectra. In ^{251}Cf, the observed $\frac{5}{2}$-$\frac{9}{2}$ level energy difference is 105.0 keV. The ^{248}Cm$(d,p)^{248}$Cm spectrum includes peaks that define level energies of 528 ± 3 and 634 ± 2 keV, which have an energy difference of 106 ± 4 keV. We have evidence for the existence of a level at 529.58 ± 0.04 keV with possible spin and parity of $\frac{3}{2}^+$ and $\frac{5}{2}$. We assign a $\frac{5}{2}^+$, $\frac{5}{2}$[622] spin, parity, and configuration to the 529.58 keV level. With the 634 keV level observed in the (d,p) spectrum assigned to the $I=\frac{9}{2}$ member of this rotational band, the $I=\frac{7}{2}$ level is expected to occur at approximately 576 keV. We find evidence for a level at 578.43 keV that deexcites to the $I=\frac{7}{2}$ member of the ground state band.

$\frac{1}{2}^-$[761]. There is strong experimental evidence for the levels at 470.21 and 494.49 keV (see Fig. 1). Model-independent arguments indicate odd parity for these levels. Examination of a Nilsson diagram[19] shows that the lowest-lying odd parity state with $\Omega=\frac{1}{2}$ or $\frac{3}{2}$ in ^{249}Cm is the $\frac{1}{2}^-$[761] configuration; it originates from the splitting of an $h_{11/2}$ spherical state. The theoretical values for the decoupling parameter are strongly negative (Table V) which means the $I=\frac{3}{2}$ level energy is expected to be less than the $I=\frac{1}{2}$ level energy. The pattern of gamma rays deexciting the 470 and 494 keV levels (Table VII) is suggestive of this sequence. The 470 keV level deexcites to the $I=\frac{1}{2}$, $\frac{3}{2}$, and $\frac{5}{2}$ levels of the ground-state band with most of the strength going to the $I=\frac{1}{2}$ and $\frac{5}{2}$ members. The 494 keV level deexcites only to the $I=\frac{1}{2}$ and $\frac{3}{2}$ levels.

BCEF observed three levels at 469, 498, and 575 keV and assigned them to the $I=\frac{3}{2}$, $\frac{7}{2}$, and $\frac{11}{2}$ levels of a band whose configuration they labeled $\frac{1}{2}^-$[750], although most references designate the configuration as $\frac{1}{2}^-$[761]. The distinguishing characteristics of the $\frac{1}{2}^-$[761] configuration are a large, negative value for the decoupling parameter and spectroscopic factors for the (d,p) reaction that indicate strong population of the $I=\frac{7}{2}$, $\frac{3}{2}$, and $\frac{1}{2}$ members of the band, in order of decreasing strength.

Thus, good experimental evidence exists to support assignment of a $\frac{1}{2}^-$[761] configuration to levels at 470.21($\frac{3}{2}$), 494.49($\frac{1}{2}$), 498($\frac{7}{2}$), and 575($\frac{11}{2}$) keV. From the three lowest energy levels, we calculate rotational parameters of $A=4.39\pm0.30$ keV and $a=-2.84\pm0.13$. This low value for A and the fact that the four experimental level energies do not fit the simple formula for rotational bands suggest the band is perturbed due to Coriolis force interaction with nearby rotational bands. We expect to observe the $I=\frac{5}{2}$ level of this band and have assigned this configuration to the level at 546.86 keV.

$\frac{3}{2}^-$[752]. The 772.74-keV level decays strongly to levels in the $\frac{1}{2}^-$[761] band; gamma decay to the $\frac{1}{2}^-$[761] band is favored by a factor of 700 over that to the $\frac{1}{2}^+$[620] ground state band (see Table VII). In the scheme of Fig. 1 this level has assigned to it possible spin and parity values of $\frac{1}{2}^+$, $\frac{3}{2}$ and $\frac{5}{2}^+$. We assign it $I=\frac{3}{2}$, partly because it decays to each of three levels in the $\frac{1}{2}^-$[761] band with comparable transition strengths. We do not see a primary transition feeding this level; this absence may be due to the statistical nature of the thermal neutron capture process.

We assign the 772.74-keV level as the $\frac{3}{2}$ member of the $\frac{3}{2}^-$[752] configuration on the basis of (1) its energy relative to two intense peaks in the (d,p) spectrum at 870 and 1030 keV, believed to be the $\frac{7}{2}^-$ and $\frac{11}{2}^-$ band members, and (2) our ability to fit the experimental levels via a Coriolis calculation, using a reasonable set of parameters.

The $\frac{3}{2}^-[752]$ configuration is a particle state in ^{249}Cm that is expected to be populated strongly by the (d,p) reaction. If we assign two intense peaks in the (d,p) spectrum at 870±4 and 1030±7 keV to the $I=\frac{7}{2}$ and $\frac{11}{2}$ members, these levels and the 772.74 keV level $(I=\frac{3}{2})$ are a consistent set described by a rotational parameter value of $A=8.0\pm0.5$ keV. The increase in this value of A, compared with an average of 6.4 for unperturbed rotational bands, is presumably due to the Coriolis interaction, which causes a decrease in A for the $\frac{1}{2}^-[761]$ band of similar magnitude.

We expect to observe the $I=\frac{5}{2}$ level of this band and have assigned this configuration to the level at 818.89 keV.

Coriolis mixing calculation for $\frac{1}{2}^-[761]$ and $\frac{3}{2}^-[752]$ configurations. As a group, the $N=7$ configurations in ^{249}Cm are expected to interact strongly with each other via the Coriolis force. One might also expect some interaction between the $\frac{1}{2}^-[761]$ and $\frac{1}{2}^-[501]$ configurations via $\Delta N=2$ mixing when the two orbitals are very close in energy, i.e., in a region of "pseudocrossing." We have chosen not to include effects of this mixing because the level crossing in question appears to occur at higher deformation than calculated for the ^{249}Cm nucleus.

In our Coriolis calculation, the energy matrix is constructed and diagonalized. The unperturbed rotational energies are given by the equation,

$$E(I)=E_0+\hbar^2/2J[I(I+1)-K^2+\delta_{K,1/2}(-1)^{I+1/2}a(I+\tfrac{1}{2})] ,$$

where E_0 is the bandhead energy, $\hbar^2/2J$ is the rotational parameter, and a is the decoupling parameter for a $K=\frac{1}{2}$ band. The off-diagonal matrix elements are given by the equation

$$A_{KK'}=\alpha\hbar^2/2J(U_KU_{K'}+V_KV_{K'})\sqrt{(I-K)(I+K+1)}\langle K\,|\,j_+\,|\,K'\rangle .$$

The parameter α is included to permit adjustment of the strength of the Coriolis interaction. The occupation amplitudes U_K and V_K are included to allow for the effect of pairing correlations. The intrinsic matrix elements are calculated by use of the CJ code.[18]

Calculations of the perturbed level structure in the rotational bands with configurations $\frac{1}{2}^-[761]$ and $\frac{3}{2}^-[752]$ were made by use of a computer code, CORMIX.[26] The program solves the secular equation for all values of angular momentum involved and uses an iterative procedure to adjust all of the variable parameters simultaneously until a best fit to the experimental level energies is obtained. Our calculations are summarized in Table VIII. The 9 level energies were fit in the calculation with a standard deviation of ±1.0 keV. Variable parameters in this calculation were the two bandhead energies, a value for the rotational parameter common to both bands, the decoupling parameter for the $\frac{1}{2}^-[761]$ band, and the parameter α which is used to attenuate the strength of the Coriolis interaction.

From our calculation we derive an experimental value for the decoupling parameter, $a=-1.89$, whose absolute value is considerably lower than the best theoretical estimate, $a=-3.36$ (Table V). Theoretically, this configuration in ^{249}Cm is calculated to possess appreciable collective nature[23]; the effect of this configuration mixing would be to lower the absolute value of the decoupling parameter. Also, the Coriolis matrix element was reduced to 86% of theoretical in order to obtain a best fit to experiment. The necessity for this reduction has been observed before for many nuclei in various regions of deformation. Recent theoretical treatments of this phenomenon[27] appear to be promising with respect to quantitative predictions of what has been treated, in the past, as a purely empirical factor in Coriolis mixing calculations.

Some of the assignments of levels with higher angular momentum in these two bands are based upon data from the (d,p) study of BCEF. We have calculated values for the appropriate cross sections (Table VIII) according to the well-established theoretical treatment for this reaction given, for example, by BCEF. In this approximation, the differential cross section is given by the equation

$$\frac{d\sigma_J^K}{d\Omega}=(2J+1)\theta_J^{\rm DW}S_J^K ,$$

where J is the total spin of the state populated and K denotes the specific state being populated. The factor $\theta_J^{\rm DW}$ was computed by use of the distorted-wave Born-approximation code DWUK72.[28] In this calculation, the optical-model parameter set of Grotdal *et al.*[29] was employed. The spectrographic

TABLE IX. Summary of experimental data for $\frac{1}{2}^-$[501] rotational bands in actinide nuclei.

Nuclide	Bandhead energy (kev)	$E_{3/2}-E_{1/2}$	A (keV)	a	Reaction/Reference
^{227}Ra$_{139}$	675.9	55.8	9.95	+0.87	$(n,\gamma)(d,p)(t,d)$
					β decay[u]
^{229}Th$_{139}$	535.5				(d,t)[m]
^{231}Th$_{141}$	554.7	38.9	6.7	+0.93	(d,t)[j,b]
					(n,γ)[q]
^{233}Th$_{143}$	539.6	46.5			$(d,p)(n,\gamma)$[i]
					(n,γ)[t]
^{233}U$_{141}$	572				(d,t)[o]
^{235}U$_{143}$	658.9	44.8			(d,p)[c]
					$(d,t)(n,\gamma)$[k]
					(n,γ)[r]
^{237}U$_{145}$	865.0	44.3			$(d,t)(^3\mathrm{He},\alpha)$[b,d]
					(n,γ)[s]
^{239}U$_{147}$	932.9	28.9			$(d,p)(n,\gamma)$[g,a]
					(n,γ)[p]
^{237}Pu$_{143}$	545	46			(d,t)[l]

factor S_J^K was computed for single particle states by use of normalized eigenvector amplitudes, $C_{i\Omega}$, as calculated with the CJ code. We compare the experimental and theoretical differential cross sections in Table VIII. Included in the comparison are cross sections calculated with the mixed single particle wave functions. We note that the calculated values tend to be smaller than experimental. Use of the mixed wave functions does not improve the fit to experiment.

$\frac{1}{2}^-$[501]. We observe levels at 917.49 and 963.00 keV that are assigned to the configuration $\frac{1}{2}^-$[501]. The 963-keV level decays to the $I=\frac{1}{2}$ and $\frac{5}{2}$ members of the ground state and, therefore, is given an $I=\frac{3}{2}$ assignment. The 917-keV level is assumed to be the $I=\frac{1}{2}$ level of this band; the most intense gamma ray deexciting this level populates the $I=\frac{3}{2}$ member of the ground-state band. Also, the 971 keV is assigned as the $I=\frac{5}{2}$ member of this band based upon this proximity to the other levels and its deexcitation to levels at 110.17 keV ($\frac{7}{2}^+$) and 529.58 keV ($\frac{5}{2}^+$). All of the transitions deexciting the 917-, 963-, and 971-keV levels are consistent with the assigned angular momentum values $I=\frac{1}{2}$, $\frac{3}{2}$, and $\frac{5}{2}$, respectively.

From the experimental level energies, we calculate values for the rotational parameter and the decoupling parameter of $A=8.41\pm0.002$ keV and $a=+0.810\pm0.002$, respectively. The theoretical value, $a=+0.76$, calculated with a Woods-Saxon potential (Table V), is in reasonable agreement with experiment.

Gareev *et al.*[23] predict an excitation of 920 keV for an $\Omega^\pi=\frac{1}{2}^-$ band whose wave function is 65% single particle character, $\frac{1}{2}^-$[501], with the next most important contributions from single particle-quadrupole vibration coupling (Table V). Our observation agrees well with the calculated properties of this configuration.

The $\frac{1}{2}^-$[501] configuration, a hole state in ^{249}Cm, has been identified in 15 odd-neutron actinides, from ^{227}Ra$_{139}$ to ^{249}Cm$_{153}$. A summary of these observations is given in Table IX. Often, it has been identified by use of (d,t) reaction spectroscopy. Although BCEF have observed a 915 keV level in their (d,p) measurement for ^{249}Cm, we doubt they are detecting the 917.47 keV level because apparently there is insufficient (d,p) strength to permit observation of this configuration in lighter nearby Cm isotopes.

The experimental $\frac{1}{2}^-$[501] bandhead energies for nuclides in this mass region are plotted in Fig. 4. These are compared with the calculated values of Soloviev and co-workers[23,30] in the figure and there is good agreement between calculation and experiment. In these calculations, Soloviev *et al.* have considered states that are predominantly quasiparticle in nature and have included the interaction between quasiparticles and phonons. The $\frac{1}{2}^-$[501] configuration has been identified in many nuclides over a range of 14 units of neutron number and it is

TABLE IX. (*Continued.*)

Nuclide	Bandhead energy (keV)	$E_{3/2}-E_{1/2}$	A (keV)	a	Reaction/Reference
$^{241}Pu_{147}$	964.7	44			$(d,p)(d,d')$[h] (d,t)[f]
$^{243}Pu_{149}$	905.9	41.3			$(d,t)(n,\gamma)$[n]
$^{243}Cm_{147}$	729	40			(d,t)[e]
$^{245}Cm_{149}$	913	43			$(d,p)(d,t)$[e]
$^{247}Cm_{151}$	958	44			(d,t)[e]
$^{249}Cm_{153}$	917.5	45.5	8.4	+0.81	(n,γ)[v]

[a]R. K. Sheline, W. N. Shelton, T. Udagawa, E. T. Jurney, and H. T. Krotz, Phys. Rev. 151, 1011 (1966).
[b]J. S. Boyno, T. W. Elze, and J. R. Huizenga, Nucl. Phys. A157, 263 (1970).
[c]T. H. Braid, R. R. Chasman, J. R. Erskine, and A. M. Friedman, Phys. Rev. C 1, 275 (1970).
[d]T. von Egidy, T. W. Elze, and J. R. Huizenga, Nucl. Phys. A145, 306 (1970).
[e]T. H. Braid, R. R. Chasman, J. R. Erskine, and A. M. Friedman, Phys. Rev. C 4, 247 (1971).
[f]T. W. Elze and J. R. Huizenga, Phys. Rev. C 3, 234 (1971).
[g]L. M. Bollinger and G. E. Thomas, Phys. Rev. C 6, 1322 (1972).
[h]T. H. Braid, R. R. Chasman, J. R. Erskine, and A. M. Friedman, Phys. Rev. C 6, 1374 (1972).
[i]T. von Egidy, O. W. B. Schult, D. Rabenstein, J. R. Erskine, O. A. Wasson, R. E. Chrien, D. Breitig, R. P. Sharma, H. A. Baader, and H. R. Koch, Phys. Rev. C 6, 266 (1972).
[j]T. Grotdal, J. Linstand, K. Nybo, K. Skar, and T. F. Thorsteinsen, Nucl. Phys. A189, 592 (1972).
[k]F. A. Rickey, E. T. Jurney, and H. C. Britt, Phys. Rev. C 5, 2072 (1972).
[l]T. Grotdal, L. Loset, K. Nybo, and T. F. Thorsteinsen, Nucl. Phys. A211, 541 (1973).
[m]T. H. Braid, J. R. Erskine, and A. M. Friedman (unpublished); reference in R. R. Chasman, I. Ahmad, A. M. Freidman, and J. R. Erskine, Rev. Mod. Phys. 49, 833 (1977).
[n]R. F. Casten, W. R. Kane, J. R. Erskine, A. M. Friedman, and D. S. Gale, Phys. Rev. C 14, 912 (1976).
[o]M. W. Johnson, R. C. Thompson, and J. R. Huizenga, Phys. Rev. C 17, 927 (1978).
[p]H. G. Börner, H. R. Koch, H. Seyfarth, T. von Egidy, W. Mampe, J. A. Pinston, K. Schreckenbach, and D. Heck, Z. Phys. A 286, 31 (1978).
[q]D. H. White, G. Barreau, H. G. Börner, W. F. Davidson, R. W. Hoff, P. Jeuch, W. Kane, K. Schreckenbach, T. von Egidy, and D. D. Warner, *Neutron Capture Gamma-Ray Spectroscopy,* edited by R. E. Chrien and W. R. Kane (Plenum, New York, 1978), p. 802.
[r]J. Almeida, T. von Egidy, P. H. M. Van Assche, H. G. Börner, W. F. Davidson, K. Schreckenbach, and A. I. Namenson, Nucl. Phys. A315, 71 (1979).
[s]T. von Egidy, J. A. Cizewski, C. M. McCullagh, S. S. Malik, M. L. Stelts, R. E. Chrien, D. Breitig, R. F. Casten, W. R. Kane, and G. J. Smith, Phys. Rev. C 20, 944 (1979).
[t]P. Jeuch, T. von Egidy, K. Schreckenbach, W. Mampe, H. G. Börner, W. F. Davidson, J. A. Pinston, and R. Roussille, Nucl. Phys. A317, 363 (1979).
[u]T. von Egidy, G. Barreau, H. G. Börner, W. F. Davidson, J. Larysz, D. D. Warner, P. H. M. Van Assche, K. Nybo, T. F. Thorsteinsen, G. Lovhoiden, E. R. Flynn, J. A. Cizewski, R. K. Sheline, D. Decman, D. G. Burke, G. Sletten, N. Kaffrell, W. Kurcewicz, T. Björnstad, and G. Nyman, Nucl. Phys. A365, 26 (1981).
[v]This work.

a hole state in all of these nuclides. Yet, its excitation energy increases by less than 500 keV over this range. This can be understood by noting that the $\frac{1}{2}^-[501]$ neutron configuration is a strongly upsloping orbital. Also there is a trend for increasing deformation of the ground state in going from ^{229}Th ($\epsilon_2=0.18$, $\epsilon_4=-0.06$) to ^{249}Cm ($\epsilon_2=0.22$, $\epsilon_4=0.0$). Thus, the effect of the increasing single-particle energy will offset the effect of the rising Fermi surface so that the change in *excitation* energy will be less than that for some of the other orbitals.

It appears from the data in Table IX that another characteristic of the $\frac{1}{2}^-[501]$ configuration is a large value for the rotational parameter, A, or a low value for the moment of inertia, although there are just three instances where rotational parameters have been determined. It may be that a low moment of inertia is characteristic of a single particle orbital such as $\frac{1}{2}^-[501]$, whose potential energy increases rapidly with increasing deformation. Niel-

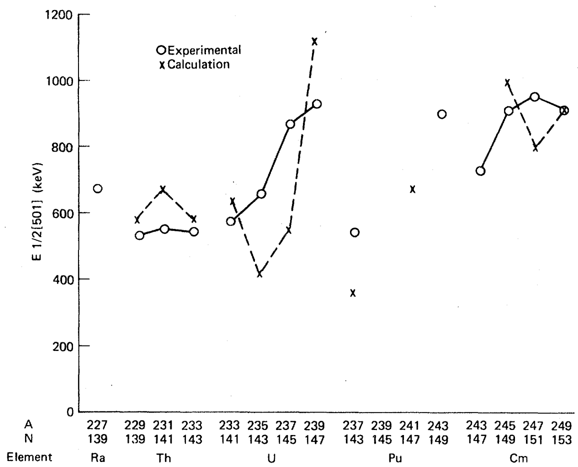

FIG. 4. Excitation energy of the $\frac{1}{2}^-$[501] odd-neutron configuration in radium, thorium, uranium, plutonium, and curium nuclei ($N=139-153$). The calculated values are those of Soloviev's group (Refs. 23 and 30). The states plotted here are predominantly one quasiparticle in nature.

sen and Bunker[31] have discussed the fact that equilibrium deformation depends upon which orbitals are occupied and have estimated that the effect on the rotational parameter caused by a change in deformation is given by the expression $(\hbar^2/2J)\alpha\epsilon_2{}^{-2}$. With these ideas we can deduce a decrease in the ϵ_2 quadrupole deformation parameter for ^{249}Cm in the $\frac{1}{2}^-$[501] configuration of 12% versus deformation in its ground state; thus, $\epsilon_2 \simeq 0.19$ in this excited state as compared with 0.22 in the ground state.

V. CONCLUSIONS

As a result of our measurements, we have extended the knowledge of the ^{249}Cm level structure up to energies of approximately 1300 keV. Of the observed gamma transitions, 52 are placed in the level scheme to define 22 excited levels. We have made three new configuration assignments: $\frac{5}{2}^+$[622], 529.58 keV; $\frac{3}{2}^-$[752], 772.74 keV; and $\frac{1}{2}^-$[501], 917.49 keV.

Some of the configurations appear experimentally at energies much below those calculated, most notably the $\frac{5}{2}^+$[622], $\frac{3}{2}^-$[752], and $\frac{1}{2}^-$[501] bands. Much of this energy decrease appears to be due to mixing of the quasiparticle state with vibrational components; e.g., the wave function for the $\frac{3}{2}^-$[752] state at 772 keV is calculated to contain only 37% of the primary single-particle configuration while octupole vibrational states coupled to two lower configurations represent 47% of the total.

A particularly outstanding difference between two types of calculation is found for the excitation energy of the $\frac{1}{2}^-$[501] configuration. In the calculations of Gareev *et al.*,[23] this state is predicted at 920 keV; its primary single-particle configuration is 65% of the wave function with most of the remainder described as gamma vibrational components built on the $\frac{1}{2}^-$[761] and $\frac{3}{2}^-$[752] configurations. A modified oscillator potential calculation puts this band at extremely high energy, ~2500 keV. We find three levels whose characteristics are appropriate for assignment to the $\frac{1}{2}^-$[501] state; the bandhead energy is 917 keV.

From our results, one can conclude that the calculations made by Soloviev's group[23] for level structure in actinide nuclei agree quite well with experiment and are the preferred calculations for comparison with other experimental studies in this deformed region.

ACKNOWLEDGMENTS

The authors are especially grateful to E. H. Kobisk and T. Quinby (ORNL) for solving the difficult problem of fabricating a GAMS target that would provide for containment, to A. F. Diggory, R. W. Lougheed, and G. Schmid for assistance in the experimental measurements, and to R. G. Lanier for expert guidance in making DWUCK calculations. The authors acknowledge the support of the U. S. Department of Energy, Office of Basic Energy Sciences and Transplutonium Program Committee in making the ^{248}Cm target material available for this experiment. One of us (R.W.H.) wishes to thank the Institut Laue-Langevin (ILL) for support during his stay in Grenoble and to thank R. J. Borg and C. Gatrousis for their continuing support of this experimental project. This work was performed under the auspices of the U. S. Department of Energy by the Lawrence Livermore National Laboratory under Contract No. W-7405-ENG-48.

*Present address: Division of Physics, National Research Council of Canada, Ottawa, Ontario K1A 0R6, Canada.

†Present address: Physics Department, Brookhaven National Laboratory, Upton, New York 11973.

‡Present address: Physics Department, Technical University Munich, D-8046 Garching near Munich, Germany.

[1]R. R. Chasman, I. Ahmad, A. M. Friedman, and J. R. Erskine, Rev. Mod. Phys. 49, 833 (1977).

[2]T. von Egidy, J. Almeida, G. Barreau, H. G. Börner, W. F. Davidson, R. W. Hoff, P. Jeuch, K. Schreckerbach, D. D. Warner, and D. H. White, Phys. Lett. 81B, 281 (1979).

[3]T. H. Braid, R. R. Chasman, J. R. Erskine, and A. M. Friedman, Phys. Rev. C 4, 247 (1971).

[4]C. E. Bemis, Jr. and J. Halperin, Nucl. Phys. A121, 433 (1968).

[5]R. Hoff, W. Davidson, D. Warner, K. Schreckenbach, H. Börner, A. Diggory, and T. von Egidy, *Proceedings of the 3rd International Symposium on Neutron Capture Gamma-Ray Spectroscopy and Related Topics, 1978* (Plenum, New York, 1979), p. 626.

[6]H. R. Koch, H. G. Börner, J. A. Pinston, W. F. Davidson, J. Faudon, R. Roussille, and D. W. B. Schult, Nucl. Instrum. Methods 175, 401 (1980).

[7]H. G. Börner, W. F. Davidson, J. Almeida, J. Blachot, J. A. Pinston, and P. H. M. Van Assche, Nuclear Instrum. Methods 164, 579 (1979).

[8]E. G. Kessler, R. D. Deslattes, A. Henins, and W. C. Sauder, Phys. Rev. Lett. 40, 171 (1978).

[9]G. Barreau, H. G. Börner, W. F. Davidson, R. W. Hoff, P. Jeuch, J. Larysz, K. Schreckenbach, T. von Egidy, and D. H. White, *Proceedings of the 3rd International Symposium on Neutron Capture γ-Ray Spectroscopy and Related Topics, Brookhaven, 1978* (Plenum, New York, 1979), p. 552.

[10]R. W. Hoff, J. E. Evans, L. G. Mann, J. F. Wild, and R. W. Lougheed, Bull. Am. Phys. Soc. 16, No. 4, 494 (1971); Nuclear Data Sheets B18, 400 (1976); B18, 407 (1976); C. W. Reich, R. G. Helmer, and R. J. Gehrke, Phys. Rev. C 19, 188 (1979).

[11]A. F. M. Ishaq, A. H. Colenbrander, and T. J. Kennett, Can. J. Phys. 50, 2845 (1972).

[12]M. L. Stelts and R. E. Chrien, Nucl. Instrum. Methods 155, 253 (1978); private communication.

[13]J. Blachot and C. Fiche, At. Data Nucl. Data Tables 20, 241 (1977).

[14]A. H. Wapstra and K. Bos, At. Data Nucl. Data Tables 19, 215 (1977).

[15]A. Bohr, and B. R. Mottelson, *Nuclear Structure* (Benjamin, Reading, Mass., 1969), Vol. I; *Nuclear Structure* (Benjamin, Reading, Mass., 1975), Vol. II.

[16]S. G. Nilsson, K. Dan. Vidensk. Selsk. Mat. Fys. Medd. 29, No. 16 (1955); B. R. Mottleson and S. G. Nilsson, K. Dan. Vidensk. Selsk. Mat. Fiz. Skr. 1, No. 8 (1959).

[17]R. D. Woods and D. S. Saxon, Phys. Rev. 95, 577 (1954); P. E. Nemirovskii and V. A. Chepurnov, Yad. Fiz. 3, 998 (1966) [Sov. J. Nucl. Phys. 3, 730 (1966)].

[18]B. Nilsson, private communication.

[19]S. G. Nilsson, C. F. Tsang, A. Sobiczewski, Z. Szymanski, S. Wycech, C. Gustafson, I. L. Lamm, P. Møller, and B. Nilsson, Nucl. Phys. A131, 1 (1969).

[20]P. Møller, S. G. Nilsson, and J. R. Nix, Nucl. Phys. A229, 292 (1974).

[21]H. J. Mang, J. K. Poggenburg, and J. O. Rasmussen, Nucl. Phys. 64, 353 (1965).

[22]A. H. Wapstra and K. Bos, At. Data Nucl. Data Tables 19, 175 (1977).

[23]F. A. Gareev, S. P. Ivanova, L. A. Malov, and V. G. Soloviev, Nucl. Phys. A171, 134 (1971).

[24]A. Faessler and R. K. Sheline, Phys. Rev. 148, 1003 (1966).

[25]I. Ahmad, F. T. Porter, M. S. Freedman, R. F. Barnes, R. K. Sjoblom, F. Wagner, Jr., J. Milsted, P. R. Fields, Phys. Rev. C 3, 390 (1971); I. Ahmad, R. K. Sjoblom, R. F. Barnes, E. P. Horwitz, P. R. Fields, Nucl. Phys. A140, 141 (1970); I. Ahmad and J. Milsted, *ibid.* A239, 1 (1975).

[26]T. P. Clements, private communication.

[27]J. Rekstad and T. Engeland, Phys. Lett. 89B, 316 (1980); K. Neergard, *ibid.* 89B, 5 (1979).

[28]P. D. Kunz, private communication.

[29]T. Grotdal, L. Loset, K. Nybo, and T. F. Thorsteinsen, Nucl. Phys. A211, 541 (1973).

[30]S. P. Ivanova, A. L. Komov, L. A. Malov, and V. G. Soloviev, Izv. Akad. Nauk SSSR, Ser. Fiz. 39, 1612 (1975); A. L. Komov, L. A. Malov, and V. G. Soloviev, *ibid.* 35, 1550 (1971).

[31]B. S. Nielsen and M. E. Bunker, Nucl. Phys. A245, 376 (1975).